Submitted to Nuclear Physics

UCRL-18963
Preprint

cy. 2

SHAPE ISOMERIC STATES IN HEAVY NUCLEI

RECEIVED
RADIATION LABORATORY
OCT 29 1969
LIBRARY AND
DOCUMENTS SECTION

Chin Fu Tsang and Sven Gösta Nilsson

August 1969

AEC Contract No. W-7405-eng-48

TWO-WEEK LOAN COPY

This is a Library Circulating Copy which may be borrowed for two weeks. For a personal retention copy, call Tech. Info. Division, Ext. 5545

LAWRENCE RADIATION LABORATORY
UNIVERSITY of CALIFORNIA BERKELEY

UCRL-18963
cy. 2

DISCLAIMER

This document was prepared as an account of work sponsored by the United States Government. While this document is believed to contain correct information, neither the United States Government nor any agency thereof, nor the Regents of the University of California, nor any of their employees, makes any warranty, express or implied, or assumes any legal responsibility for the accuracy, completeness, or usefulness of any information, apparatus, product, or process disclosed, or represents that its use would not infringe privately owned rights. Reference herein to any specific commercial product, process, or service by its trade name, trademark, manufacturer, or otherwise, does not necessarily constitute or imply its endorsement, recommendation, or favoring by the United States Government or any agency thereof, or the Regents of the University of California. The views and opinions of authors expressed herein do not necessarily state or reflect those of the United States Government or any agency thereof or the Regents of the University of California.

SHAPE ISOMERIC STATES IN HEAVY NUCLEI†

Chin Fu Tsang and Sven Gösta Nilsson††

Lawrence Radiation Laboratory
University of California
Berkeley, California 94720

August 1969

Abstract

The trend for the occurrence of secondary minima (shape isomers) in the potential-energy surface is discussed for an extended region of heavy nuclei. The calculations reported are based on a modified oscillator potential, and a renormalization of the average behaviour of the total energy to that of the liquid-drop model is performed. The regions treated are the actinide region, the rare earth region along the stability line, and a region of neutron deficient isotopes of elements in the Pb region.

†Work performed under the auspices of the U. S. Atomic Energy Commission.

††On leave of absence from Lund Institute of Technology, Lund, Sweden.

1. Introduction

The fission isomers were first discovered in the experiments of Polikanov, Flerov et al.[1,2]), and they have been studied extensively in more recent experiments[3]). Several attempts have been made to identify them with the shape isomeric state corresponding to a secondary minimum (largely along the axis of quadrupole distortions) that has been found to occur in the total potential-energy surface plotted as a function of deformations. Thus instead of the conventional picture of an one-peaked energy barrier along the deformation path leading to fission, one has a two-peaked barrier where between the two peaks there is a secondary minimum at a higher energy than the ground state minimum but prevented from decaying to the ground state or fissioning by the two energy peaks.

Probably the first of the attempts to theoretically locate the minimum in this part of the potential-energy surface are the early publications of Strutinsky[4]) and Gustafson et al.[5]). The first paper treats the nuclear potential by a first-order perturbation theory, but the new and very fruitful idea of the renormalization of the total single-particle energy to the liquid-drop model by a method sometimes cited as the "Strutinsky Prescription" is there introduced. The purpose of the procedure quoted is to correct for the unrealistic behaviour of the absolute values of the total single-particle energy as a function of deformation and mass number, and it has been the method employed in all relevant subsequent calculations of the fission barrier based on the single-particle model. To describe the liquid-drop energy this paper employed an expansion in the deformation parameter ε, which has a poor convergence so that the second peak of the two-peaked barrier is somewhat

suppressed. In the second paper[5]) a weak secondary minimum can be found for a series of nuclides at about the right distortion. For computational reasons the calculation was only carried so far in distortion as to the beginning of the second peak. This paper[5]) is based on the modified oscillator model without renormalization to the liquid drop model.

2. Present Method of Calculations

The single-particle potential used in ref. [5]) has been employed in the much more realistic and more successful subsequent calculations by Nilsson et al.[6,7]). This work is paralleled by the publications of the Strutinsky group[8,9]). In all of these references the Strutinsky prescription is employed. Two degrees of freedom are considered: P_2 and P_4 distortions, measured by the coordinates ε and ε_4. Oblate and prolate shapes are represented by negative and positive ε-values, respectively. The sign of ε_4 is so defined that a positive ε_4 represents a waistline indentation relative to the spheroid shape defined by ε. The potential is given as

$$V = \frac{1}{2}\hbar\omega_o(\varepsilon,\varepsilon_4)\rho^2(1 - \frac{2}{3}\varepsilon P_2 + \varepsilon_4 P_4) + \quad (\vec{\ell}\cdot\vec{s} \text{ and } \vec{\ell}^2) \text{ terms}$$

where ρ is the radius vector length in so-called stretched coordinates[6]). In recent calculations[10,11]) also P_3 and P_6 shapes have been considered in addition to the gamma (rotationally asymmetric) degree of freedom[12]). However the ε and ε_4 coordinates presently appear to be the most relevant ones for the barrier penetration problem.

In these calculations, in accordance with the Strutinsky prescription, the averaged energy is subtracted out from the sum of the single-particle energies. The remaining energy is referred to as "the shell contribution". To this energy is then added the surface and Coulomb energy terms in the liquid-drop model with parameters taken from the papers of Myers and Swiatecki[13]). The Coulomb energy term is evaluated numerically employing a method due to Nix[14]). Pairing energy is also added, in which a surface and isospin dependent pairing matrix element is introduced[7]). In this way the total potential

energy surface is calculated as a function of deformations. Strutinsky, Muzychka and co-workers[15]) have also calculated the potential energy by a similar method. However, in their work the P_4 deformation is neglected and, so far, their calculations have been restricted to the regions of actinide and superheavy nuclei.

3. The Potential Energy Surface

In figs. 1-6 the potential energy surfaces in the $(\varepsilon,\varepsilon_4)$ plane are shown for ^{228}U, ^{242}Pu, ^{244}Cm, ^{250}Cf, ^{252}Fm and ^{254}No. One way to exhibit the fission barrier is to plot the potential energy as a function of ε with minimization of energy with respect to ε_4 for each value of ε. This type of plot represents a cut through the two-dimensional potential surface along the potential energy minimum path with the energies projected on the ε axis.

In fig. 7 we show such a plot for the superheavy nuclides $^{298}114$ and $^{294}110$ and two actinide nuclides $^{242}94$ and $^{254}100$. From the figure we see that for a nucleus with its proton or neutron number near a magic number the ground state is spherical, $(\varepsilon=0)$, but a secondary minimum occurs at $\varepsilon \approx 0.4$. For a nucleus with its neutron and proton numbers away from the magic numbers the ground state occurs at $\varepsilon \approx 0.2 - 0.25$ and a secondary minimum occurs at $\varepsilon \approx 0.6 - 0.7$.

The existence of the two-peak structure of the potential-energy barrier is sometimes described as due to a "secondary shell effect", the "primary shell effect" being responsible for the ground-state deformations. If this effect occurs at or near the liquid-drop saddle point, the peaks will be of about equal height.

The secondary minimum is found to occur in the region of deformation $\varepsilon = 0.35$ to 0.75 depending on the N and Z values of the nucleus considered. As we go along the stability line in the periodic table from small-A to large-A nuclei, the fissility parameter x increases and the liquid-drop saddle point will move from large ε to small ε. For the rare-earth region near beta stability the liquid-drop saddle points are located beyond $\varepsilon = 1.0$, whereas in the actinide region they are located between $\varepsilon \simeq 0.5$ and $\varepsilon \simeq 0.9$. Thus it appears that the two-peaked structure in the fission barrier will be prominent in the actinide region. Another favourable region with similar x-values is that of neutron deficient nuclides with $Z \approx 82$.

4. Shape (Fission) Isomers in the Actinide Region

Fission isomers have long been observed and studied in the actinide region. In this region the corresponding single-particle graphs are available and provide a more detailed understanding of the relation between the shell crossings and the occurrence of the peaks and valleys in the fission barrier. If we follow along the Fermi level corresponding to, for instance, $N = 150$ or $Z = 100$ in figures 2k and 2ℓ of ref. [7]), we notice the following. The first strongly downward trend in the potential-energy surface along the axis of P_2 distortion (the ε-axis) is caused by the crossing of shells with $\Delta N = 1(2)$, where the figure in parenthesis refers to states from subshells pulled down by the spin-orbit force from the next shell above. After this the energy surface again obtains a positive second derivative due to the volume conservation of the harmonic-oscillator potential well. Thereby the first minimum, situated at about $\varepsilon \simeq 0.25$, is formed. The next downward trend is caused by shell crossings with $\Delta N = 2(3)$ followed by a secondary minimum in the relative absence of more crossings. This occurs at about $\varepsilon \approx 0.6 - 0.7$. Beyond that the second peak rises until the $\Delta N = 3(4)$ crossing in combination with the general liquid-drop energy fall-off again causes a downward trend.

In fig. 8 the barriers obtained for isotopes of $Z = 92$ to $Z = 100$ can be studied with the above general discussion in mind. This figure is based on a later calculation than those for figs. 1-6, representing minor improvements of the theory [7]). As explained in ref. [7]) these barrier shapes are reasonably reliable for small deformation ε. For large deformations in ε (say $\varepsilon \gtrsim 0.8$) the potential barrier is over-estimated mainly because of

our restricted parametrization of the shape. The general trends in the figure should be noted. It is in the region of Pu and Cm, whose liquid drop saddle points are coincident with the position of the secondary shell effect, that the two-peak barrier is most prominent.

In fig. 9 we exhibit theoretical half-lives for fission decay through the outer barrier peak. These half-lives have been computed in the following way. An effective experimental inertial mass parameter B_{eff} is calculated by employing the empirical ground state half-lives and our calculated barriers $W(\varepsilon)$ according to the relation

$$\tau_{1/2} \propto \exp\left[\frac{2}{\hbar}\sqrt{2B_{eff}}\int\sqrt{W(\varepsilon) - E}\,d\varepsilon\right] ,$$

where E is the zero point energy taken to have a nominal value of $\frac{1}{2}$ MeV. This same B_{eff}-value is then used to calculate the half-life for the penetration through the second barrier.

In all likelihood this procedure underestimates the effective B-value for the penetration through the second barrier, as the microscopic calculations by Sobiczewski et al.[16]) bear out. We have also tried to use rB_{eff} as the inertial parameter for the penetration through the second barrier, where r is an adjustable constant. It turns out that the average value of r is approximately unity over the whole actinide region. What this means is that on the average the underestimate of our effective B value is largely compensated for by the theoretical overestimate of the outer peak. However for $_{92}U$, where the barrier extends to very large deformations, the overestimate

of the outer barrier is not compensated by the employment of the averaged empirical inertial parameter. It is thus not surprising to find the theoretical half-lives of U isotopes somewhat too long when compared with experimental values, as is indicated in the figure. On the other hand, the barriers of Pu, Cm, Cf and Fm extend to relatively small deformations and one would hope the estimates to be more reliable in those cases. Assuming that the theoretical calculations provide with some reliance the main trends with Z and A, this figure gives a strong indication that it is very unlikely to observe the shape fission isomers in the even-even nuclei beyond Pu and Cm. The reported[17,18]) fission isomer case of ^{246}Cf is not verified by more recent experiments[19]).

The half-lives for penetration through the inner peak is, in many cases, shorter than those through the outer peak. However in almost all the cases the "subsequent" gamma-decay process is probably decisive for the actual half-lives for the mode of decay involving the inner barrier.

Besides the comparison of our theoretical fission half lives to the experimental values, one could also look at the isomer excitation energies and the barrier heights. In the cases where comparison of the excitation energy can be made, the agreement is remarkable, as shown by Lark and co-workers[3]). The highest barrier peak in the heaviest actinides is also approximately reproduced as shown in the same reference.

5. Shape (Fission) Isomers in the Neutron-Deficient Rare-Earth Region

In figs. 10-15 we exhibit our calculated fission barriers for neutron deficient isotopes of $_{80}Hg$, $_{82}Pb$, $_{84}Po$, $_{86}Rn$, $_{88}Ra$ and $_{90}Th$. It appears from these barrier shapes that the shape isomeric state would probably favor penetration through the small inner peak and subsequent gamma-decay to the ground state rather than fissioning through the much larger outer peak. Recently it is reported[20]) that fission isomers are detected in this region. An explanation may be as below.

Although the half-life for penetration through the inner peak can be estimated to be so short compared with that for the penetration through the second peak, the subsequent gamma decay process will determine the half-life of transition back into the ground state. This in turn depends on the detailed microscopic character of the collective fission state. A considerable delay may be expected which might possibly make the fission decay through the outer barrier competitive. Furthermore we have overestimated the outer peak due to insufficient parametrization. Thus while the parametrization error is negligible at $\varepsilon \leqslant 0.6$, it grows to nearly one MeV already at $\varepsilon \approx 0.85$. Until corrections have been made for this overestimate of the outer fission peak and until microscopic inertial mass parameters are available, we are forced to refrain from detailed quantitative estimates of the shape isomeric half-lives in this region.

6. Shape Isomers Along the Stability Line with $70 < Z < 90$

Extensive calculations of energy surfaces out to very large distortions have been performed by us down to $Z = 62$ for elements in the vicinity of the stability line. For the lighter of these the fissility parameter x is very small and consequently the liquid-drop barrier high and wide. Even though the shell contribution shows considerable fluctuations as a function of distortion, a real secondary minimum does not develop until about $Z = 72$ (fig. 16). Here the surface merely flattens out at an excitation of approximately 12 MeV and over a region around $\varepsilon \approx 0.5$, $\varepsilon_4 \approx 0.08$. (Note that along the ε-axis there is no trace of an isomer at all to be found.)

In fig. 17 ($Z = 76$, $A = 192$) there occurs a secondary minimum at $\varepsilon \approx 0.4$ and at an excitation energy of about 6 MeV. For $Z = 76$, $A = 198$, a somewhat neutron rich isotope of the same element (smaller x-value) with a spherical ground-state shape, the same secondary minimum shows up at 9 MeV of excitation (fig. 18). A very deep secondary minimum occurs at about 11 MeV of excitation in ^{202}Hg ($Z = 80$, $A = 202$), fig. 19. This should constitute a long-lived gamma isomer. The low side of the barrier is deep enough, ≈ 3 MeV, to contain high spin members of occurring rotational bands. (Isomeric states in this region of nuclei were noticed already in ref. [5])). A similar situation (fig. 20) occurs for ^{208}Pb ($Z = 82$, $N = 126$) but due to the very strong ground-state shell effects, the isomeric state occurs at about 16 MeV of excitation probably with a very short half-life. Very low-lying secondary minima occur for the two isotopes of ^{220,224}Ra, namely $Z = 88$, $N = 132$ and $Z = 88$, $N = 136$ exhibited in figs. 21 and 22. The secondary minima there occur at about 4 and 2 MeV of excitation, respectively. In particular the first case shows a very

substantial inner barrier and should be observable as an electromagnetic isomer. In none of the cases treated in this paragraph is fission a competitive mode of decay due to the dominance of the outer barrier. This in turn is due to the low x-values in this region of nuclei.

7. Other Possible Cases of Shape Isomeric States

Shape isomeric states are also expected to occur in the superheavy nuclei region ($Z \sim 114$, $N \sim 184$) as is obvious from ref. [7]) and fig. 7 of this present paper. Here the secondary shell effect occurs at about the flat part of the liquid drop barrier. The two-peak character of the barrier is also in this region a prominent feature, although the second peak is somewhat lower than the first one.

A large number of new shape isomeric states are expected to arise in the odd-even and odd-odd nuclei due to the odd-nucleon effects. As the condition of conservation both of parity and of angular momentum along the axis of deformation has to be upheld, the potential-energy surface is liable to exhibit an even larger number of local minima. The ones already present in the neighboring even-even cases may be considerably deeper due to the effect of the odd-particle. This contention is well borne out by calculations presently being performed[21]).

ACKNOWLEDGMENTS

The stimulating and constructive discussions with Dr. W. J. Swiatecki, and Dr. E. Cheifetz have been of great value for this work. We also gratefully acknowledge useful communications with Drs. S. G. Thompson, J. Borggreen, and S. Björnholm. The close cooperation with the Warsaw group of Drs. A. Sobiczewski, Z. Szymanski, and S. Wycech in our program is highly appreciated.

The friendly hospitality of the Nuclear Chemistry Division and its excellent publication services are gratefully acknowledged.

References

1) S. M. Polikanov, V. A. Druin, V. A. Karnaukov, V. L. Mikheev, A. A. Pleve, N. K. Skobolev, V. G. Subotin, G. M. Ter-Akopian and V. A. Fomichev, Exp. Theor. Phys. 42 (1962) 164; S. Bjørnholm, J. Borggreen, L. Westgaard and V. A. Karnaukov, Nucl. Phys. A95 (1967) 513

2) G. N. Flerov and S. M. Polikanov, Compt. Rend. Congr. Int. Phys. Nucl. (Paris 1964) Vol. I, p. 407

3) N. Lark, G. Sletten, J. Pedersen, and S. Bjørnholm, Nucl. Phys. (1969) in press, and the references quoted therein

4) V. M. Strutinsky, Lysekil Symposium, 1966, (Almqvist and Wiksell, Stockholm, 1967), p. 629, and Arkiv Fysik 36 (1967) 629

5) C. Gustafson, I. L. Lamm, B. Nilsson, and S. G. Nilsson, Lysekil Symposium, 1966, op. cit., p. 613; Arkiv Fysik 36 (1967) 613

6) S. G. Nilsson, J. R. Nix, A. Sobiczewski, Z. Szymanski, S. Wycech, C. Gustafson and P. Möller, Nucl. Phys. A115 (1968) 545

7) S. G. Nilsson, C. F. Tsang, A. Sobiczewski, Z. Szymanski, S. Wycech, C. Gustafson, I. L. Lamm, P. Möller, and B. Nilsson, Nucl. Phys. A131 (1969) 1; S. G. Nilsson, Lawrence Radiation Laboratory Report No. UCRL-18355-Rev. (Berkeley, Sept. 1968); S. G. Nilsson, S. G. Thompson, and C. F. Tsang, Phys. Letters 28B (1969) 458

8) V. M. Strutinsky, Nucl. Phys. A95 (1967) 420; V. M. Strutinsky, Nucl. Phys. A122 (1968) 1

9) V. M. Strutinsky and Zu. A. Muzychka, Proc. Int. Conf. on the Phys. of Heavy Ions, October 1966, Vol. II, 51

10) P. Möller and S. G. Nilsson, Phys. Letters, to be published

11) P. Möller and B. Nilsson, to be published.

12) V. V. Pashkevich, Conf. Int. Symp. Nucl. Symp. Nucl. Structure, Dubna (1968) 94

13) W. D. Myers and W. J. Swiatecki, Lysekil Symposium, Sweden, 1966, (Almqvist and Wiksell, Stockholm, 1967), p. 393, and Arkiv Fysik, 36 (1967) 593

14) J. R. Nix, Further studies in the liquid-drop theory of nuclear fission, appendix, University of California Lawrence Radiation Laboratory Report UCRL-17958 (July 1968)

15) Yu. A. Muzychka, Phys. Letters 28B (1969) 539

16) A. Sobiczewski, Z. Szymanski, S. Wycech, S. G. Nilsson, J. R. Nix, C. F. Tsang, C. Gustafson, I. L. Lamm, P. Möller and B. Nilsson, Nucl. Phys. A131 (1969) 67

17) Yu. P. Gangrskii, B. N. Markov, S. M. Polikanov, and H. Jungklaussen, Joint Institute of Nuclear Research R-2841, Dubna, 1966; and J.E.T.P. Letters 4 (1966) 289

18) Yu. P. Gangrskii, B. N. Markov, L. M. Polikanov, J. F. Harisov, and H. Jungklaussen, Izvest. Akad. Nauk. USSR, Phys. Ser. 32 (1968) 1644

19) H. R. Bowman, E. Cheifetz, and R. C. Gatti, private communication

20) F. H. Ruddy and J. M. Alexander, to be published

21) G. Ollén and P. Möller, to be published

22) R. Vandenbosch and K. L. Wolf, University of Washington (Seattle) International Atomic Energy Agency, 2nd Symp on Phys. and Chem. of Fission, Vienna, 28 July - 1 August 1969, Paper No. SM-122/110 (1969)

Figure Captions

Fig. 1. Total potential-energy surface of ^{228}U given as a contour map in $(\varepsilon,\varepsilon_4)$ plane[7]). The contour lines represent steps of 1 MeV.

Fig. 2. Same as fig. 1 for ^{242}Pu.

Fig. 3. Same as fig. 1 for ^{244}Cm.

Fig. 4. Same as fig. 1 for ^{250}Cf.

Fig. 5. Same as fig. 1 for ^{252}Fm.

Fig. 6. Same as fig. 1 for ^{254}No.

Fig. 7. Potential energy (solid curve) minimized with respect to ε_4 as functions of ε for various nuclei to illustrate the shell structure effects in relation to the liquid-drop background (dashed curve).

Fig. 8. The projected two-peak barrier as function of mass number for Z = 92 - 100 (see ref. [7])).

Fig. 9. Theoretical half-lives (solid curves) for fission barrier penetration of the outer peak. Experimental spontaneous fission half-lives of U isomers are shown as open triangles[3]) and circles[22]) and those of Pu isomers are shown as filled triangles[3]) and circles[22]).

Fig.10 . Total potential energy minimized with respect to ε_4 for each ε as function of ε for <u>neutron deficient</u> isotopes $_{80}Hg$. Calculations correspond to the assumption that the pairing strength is proportional to the nuclear surface area.

Fig. 11. Same as fig. 10 for <u>neutron deficient</u> isotopes of $_{82}Pb$.

Fig. 12. Same as fig. 10 for <u>neutron deficient</u> isotopes of $_{84}Po$.

Fig. 13. Same as fig. 10 for <u>neutron deficient</u> isotopes of $_{86}Rn$.

Fig. 14. Same as fig. 10 for <u>neutron deficient</u> isotopes of $_{88}Ra$.

Fig. 15. Same as fig. 10 for <u>neutron deficient</u> isotopes of $_{90}Th$.

Fig. 16. Potential-energy plot in $(\varepsilon,\varepsilon_4)$ planes for ^{174}Hf. This plot corresponds to an earlier calculation of ref. [7]), where only second-order corrections to the Strutinsky smearing function have been applied.

Fig. 17. Same as fig. 16 for ^{192}Os.

Fig. 18. Same as fig. 16 for ^{198}Os.

Fig. 19. Same as fig. 16 for ^{202}Hg.

Fig. 20 Same as fig. 16 for ^{208}Pb.

Fig. 21 Same as fig. 16 for ^{220}Ra.

Fig. 22 Same as fig. 16 for ^{224}Ra.

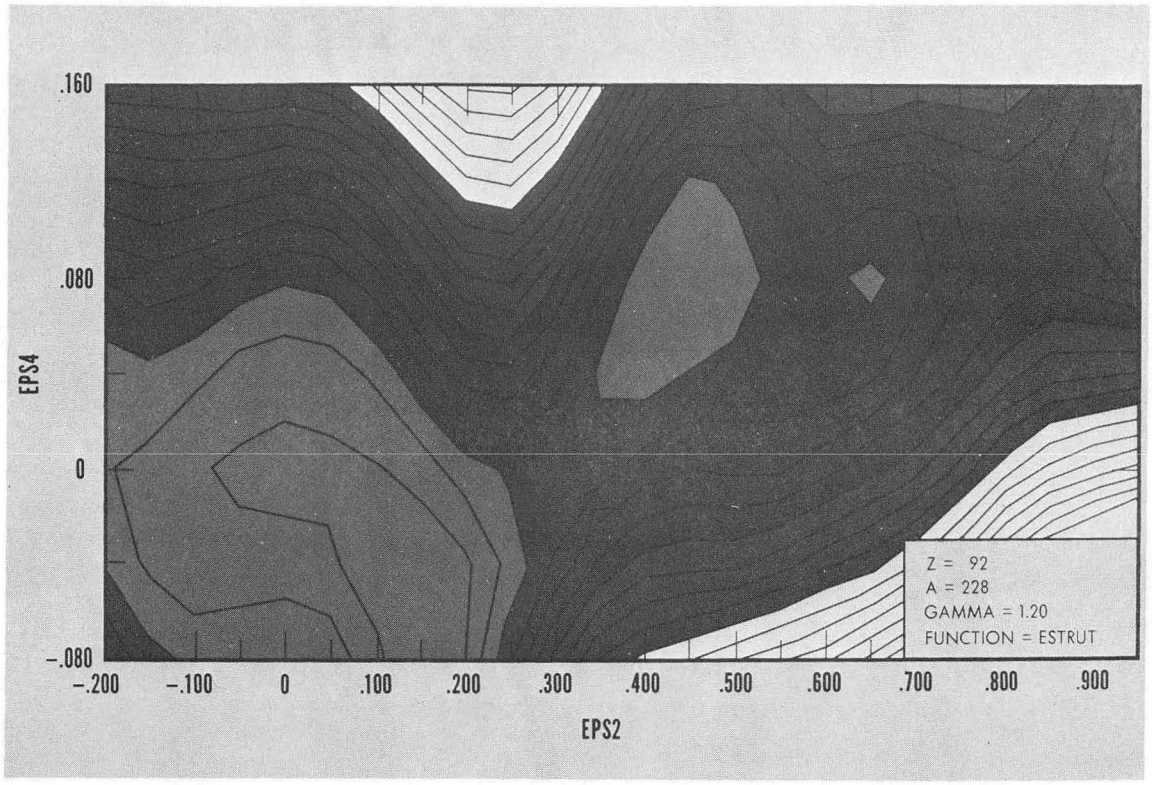

XBC 688-5119

Fig. 1

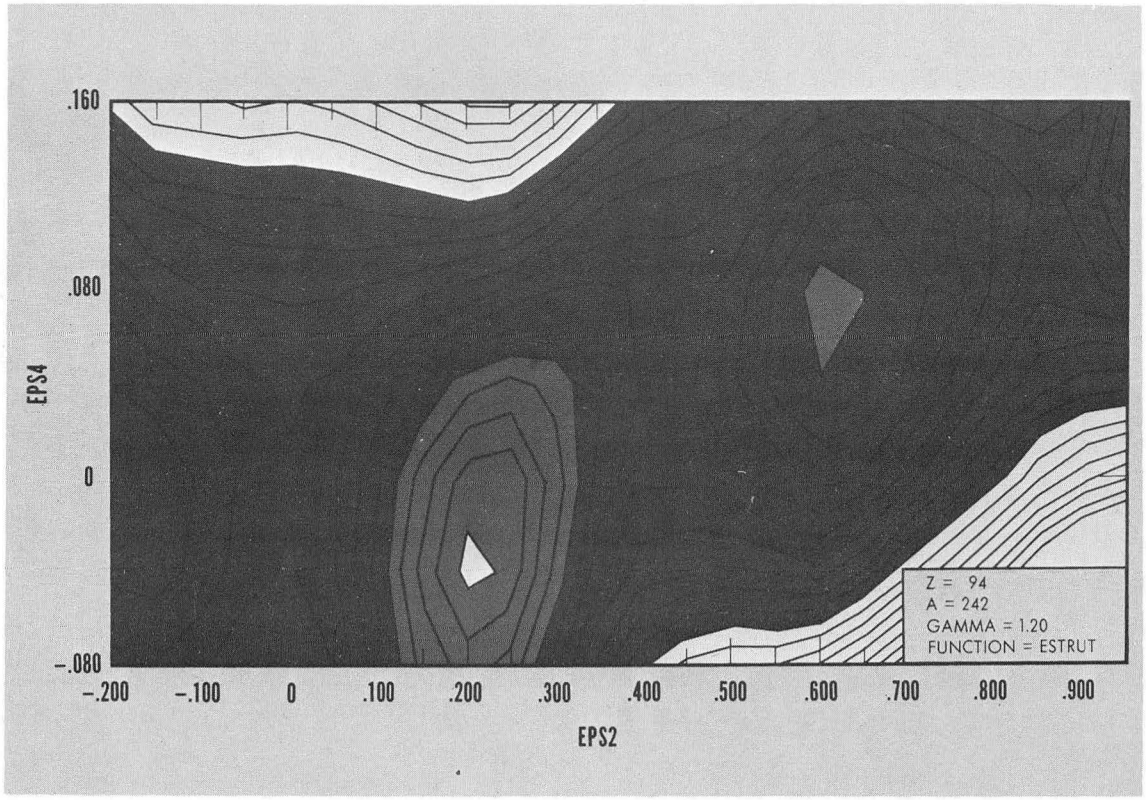

XBC 688-5121

Fig. 2

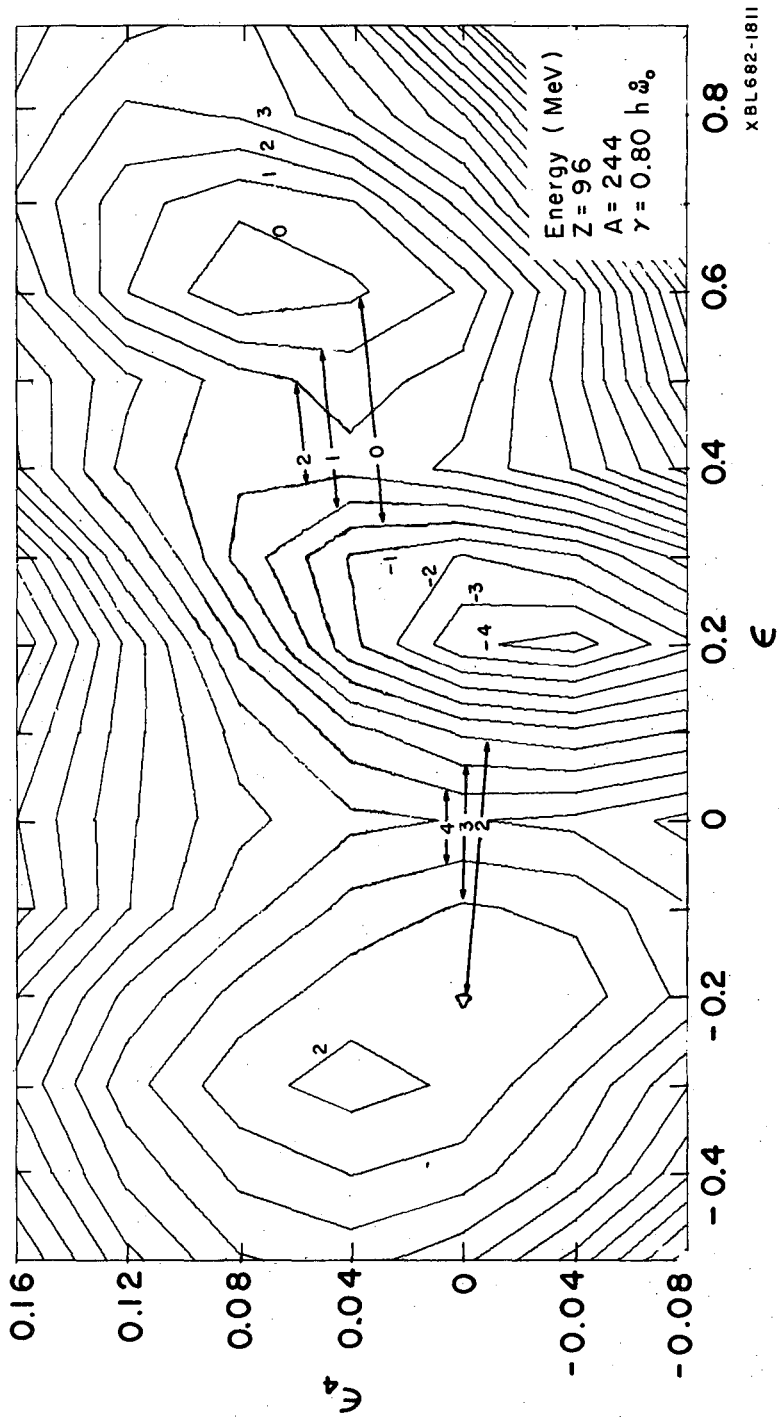
Energy (MeV)
Z = 96
A = 244
γ = 0.80 ħω₀
ε
ε₄
0.16
0.12
0.08
0.04
0
-0.04
-0.08
-0.4
-0.2
0
0.2
0.4
0.6
0.8
XBL682-1811

Fig. 3.

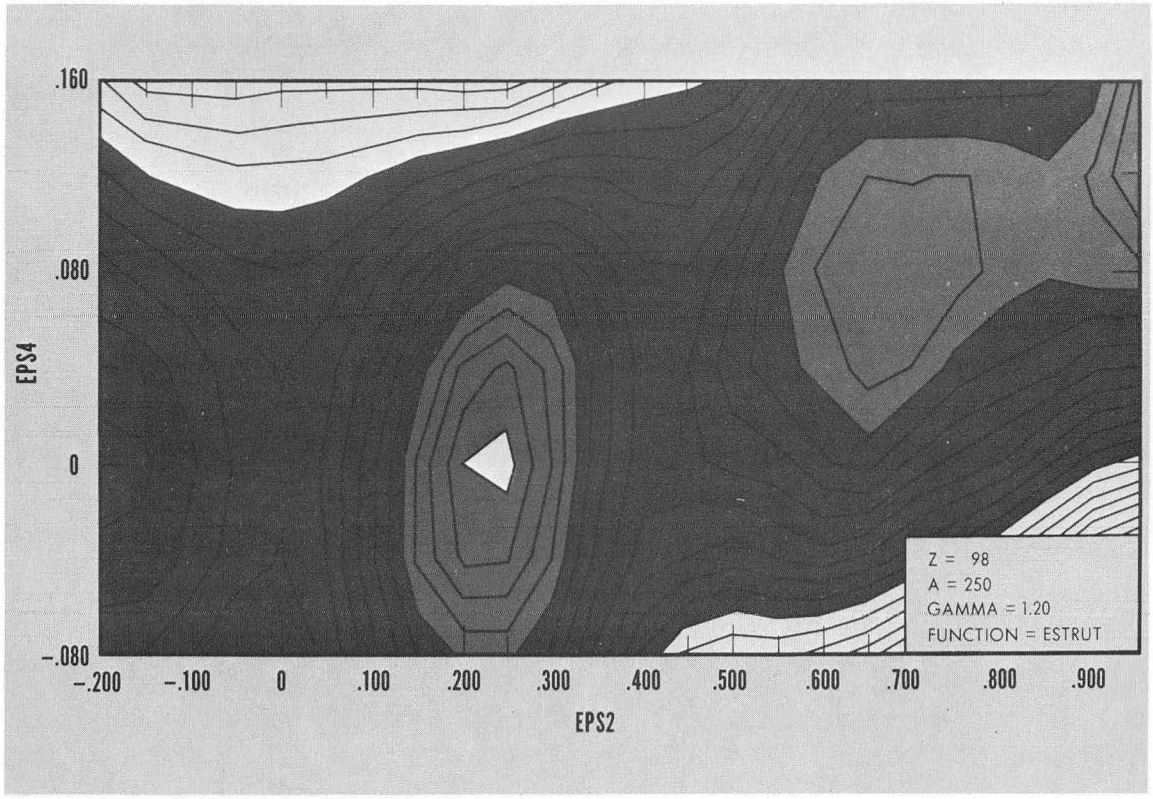

XBC 688-5120

Fig. 4

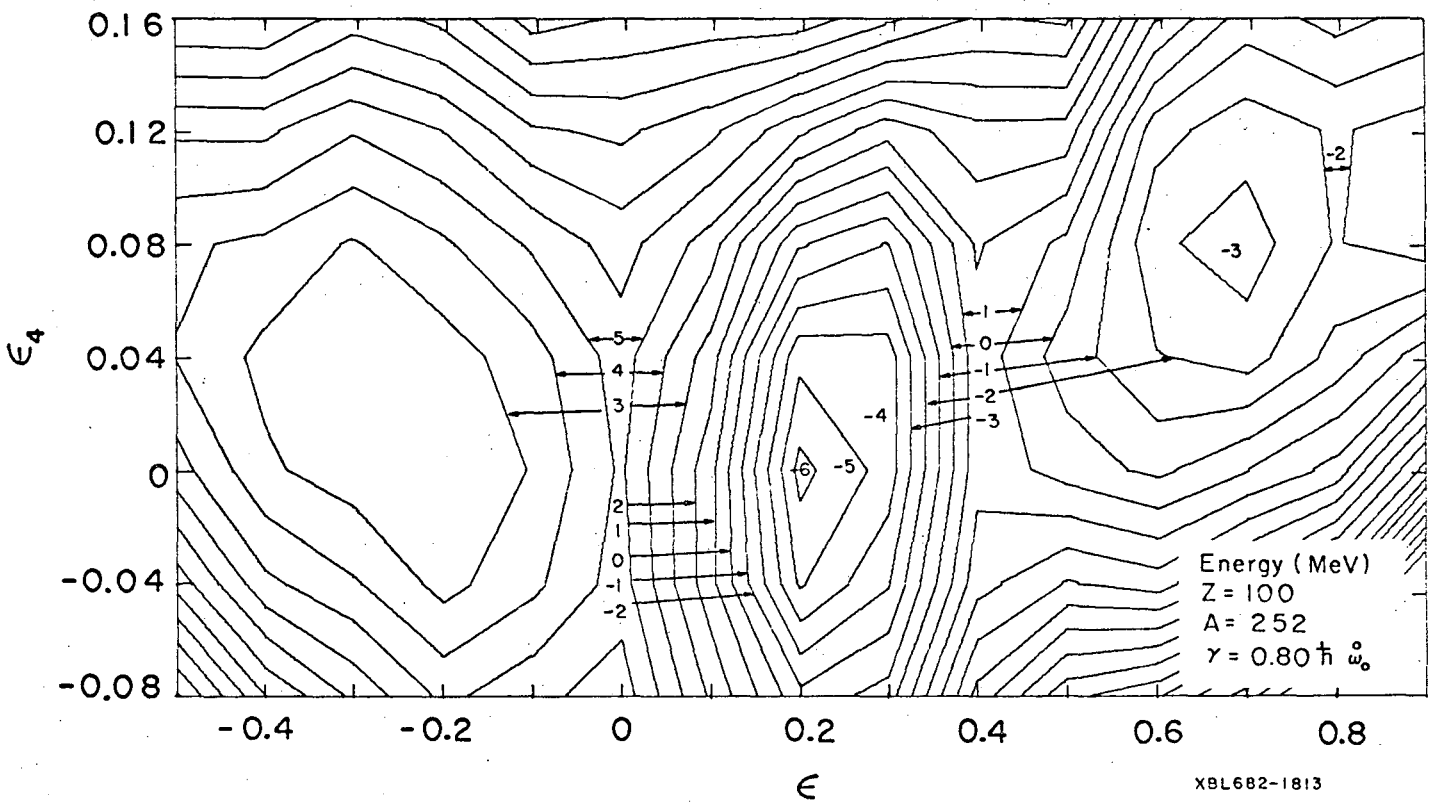
0.16
0.12
0.08
0.04
0
-0.04
-0.08
ϵ_4
-0.4
-0.2
0
0.2
0.4
0.6
0.8
ϵ
Energy (MeV)
Z = 100
A = 252
$\gamma = 0.80\hbar\,\mathring{\omega}_0$
XBL682-1813

Fig. 5.

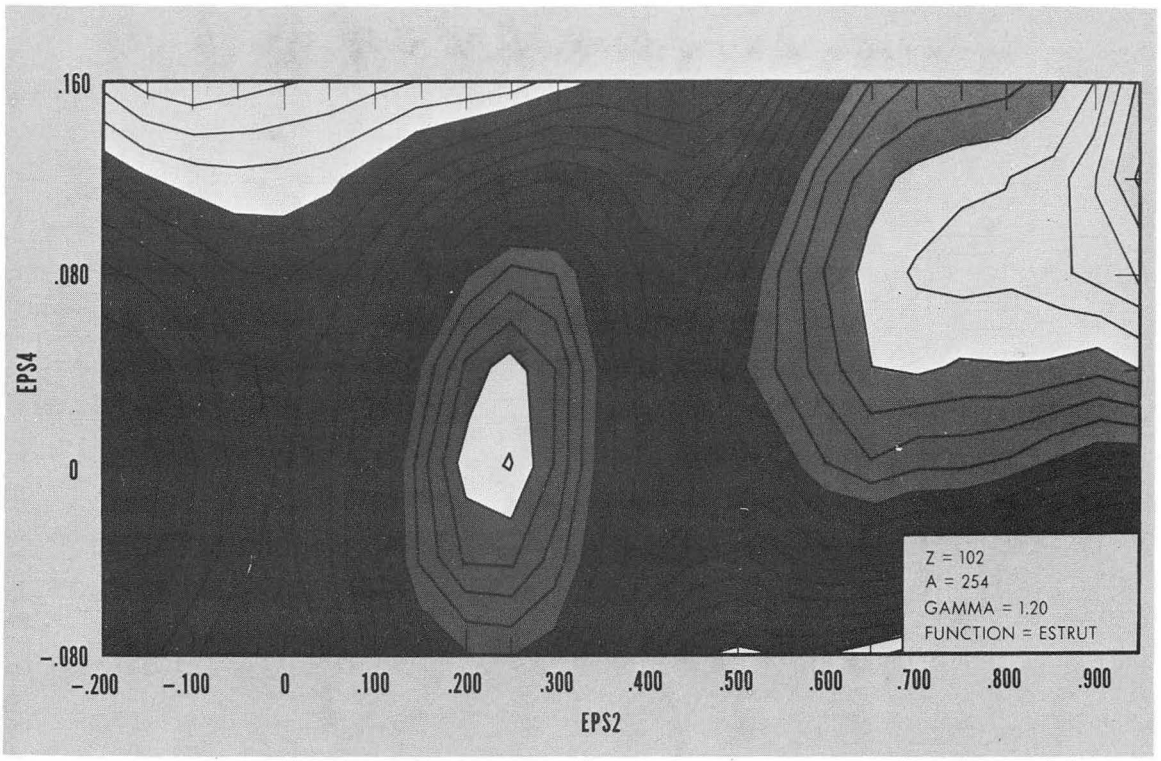

XBC 688-5116

Fig. 6

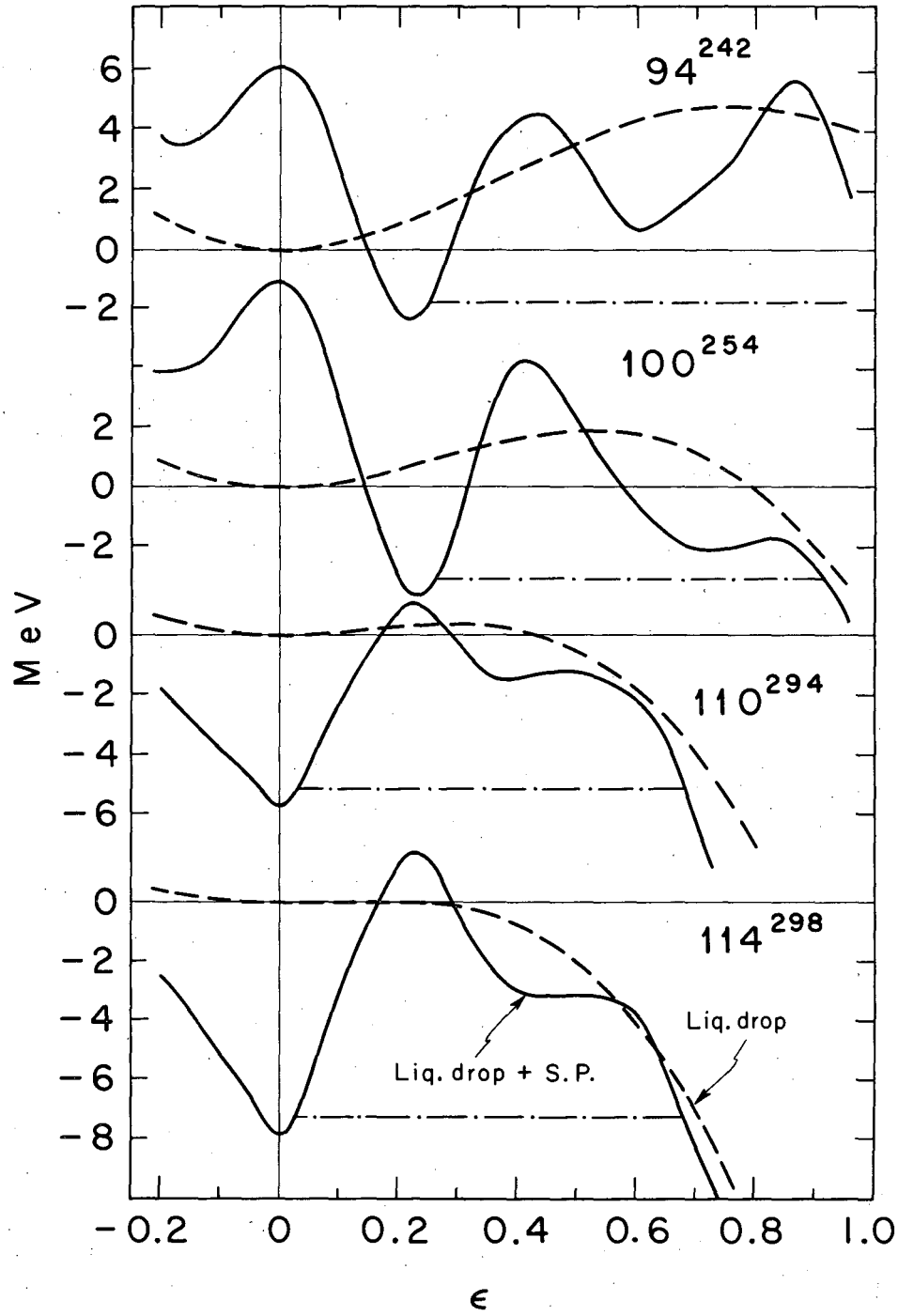

XBL688-3679

Fig. 7.

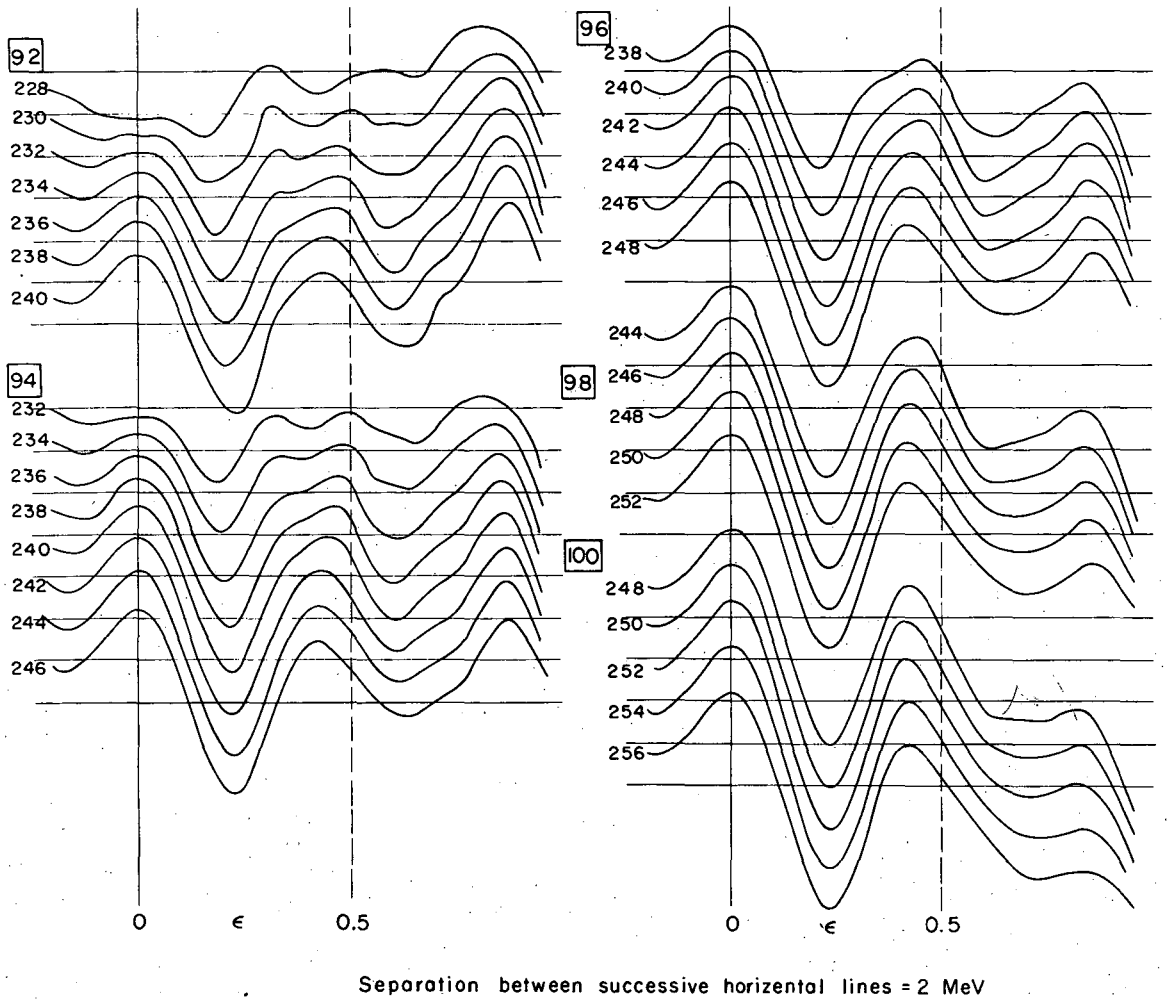

XBL691-1638

Fig. 8.

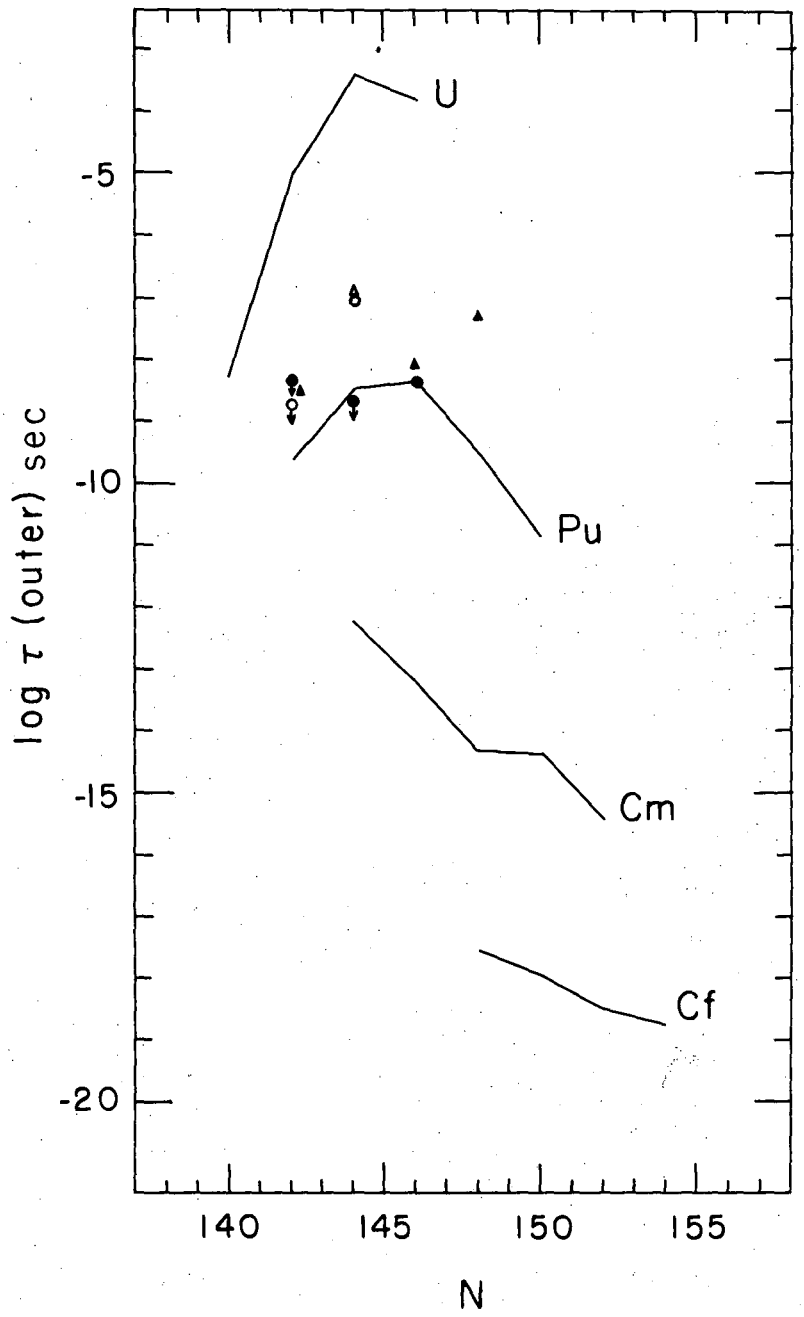

XBL 698-1387

Fig. 9.

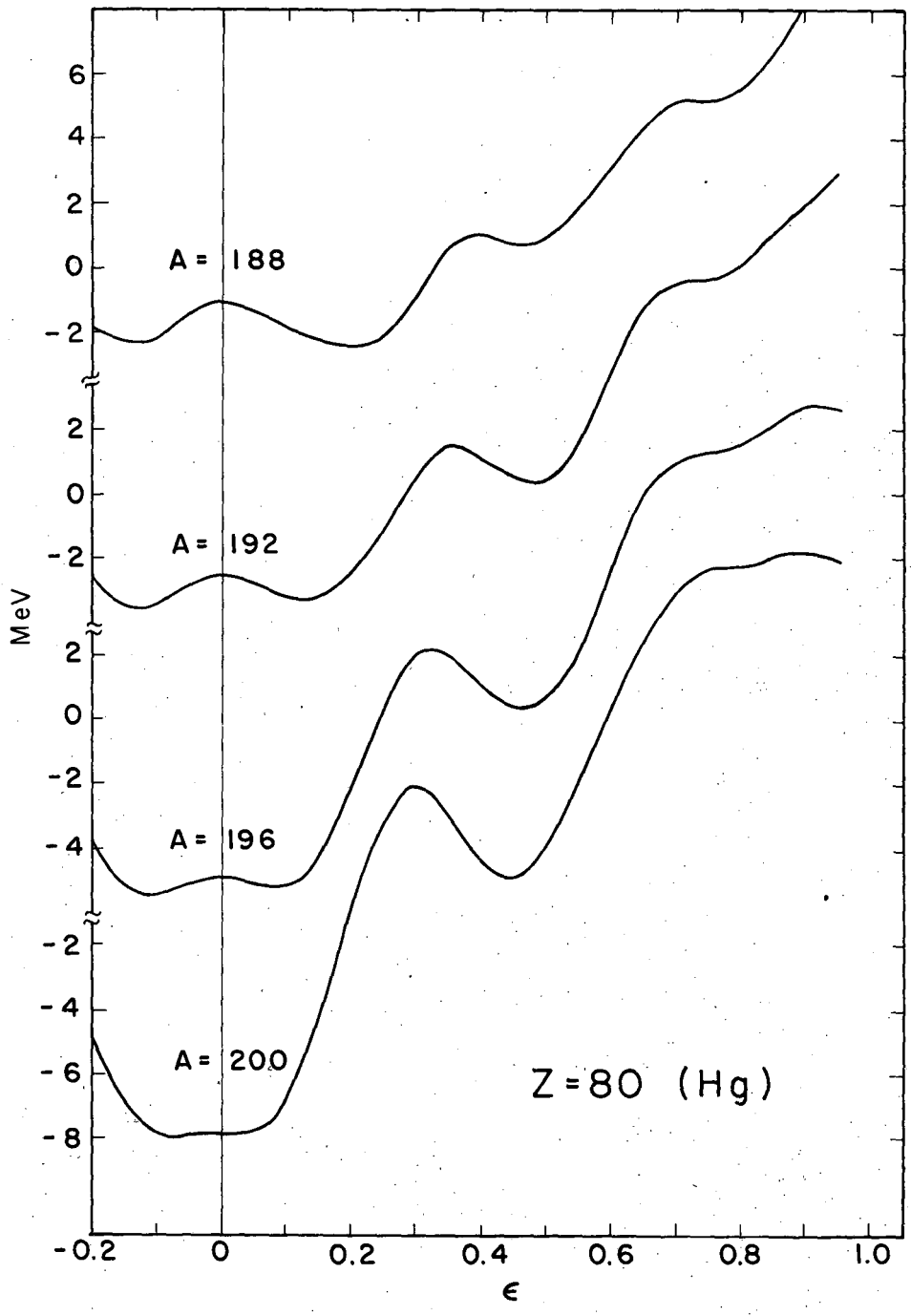

XBL693- 2257

Fig. 10.

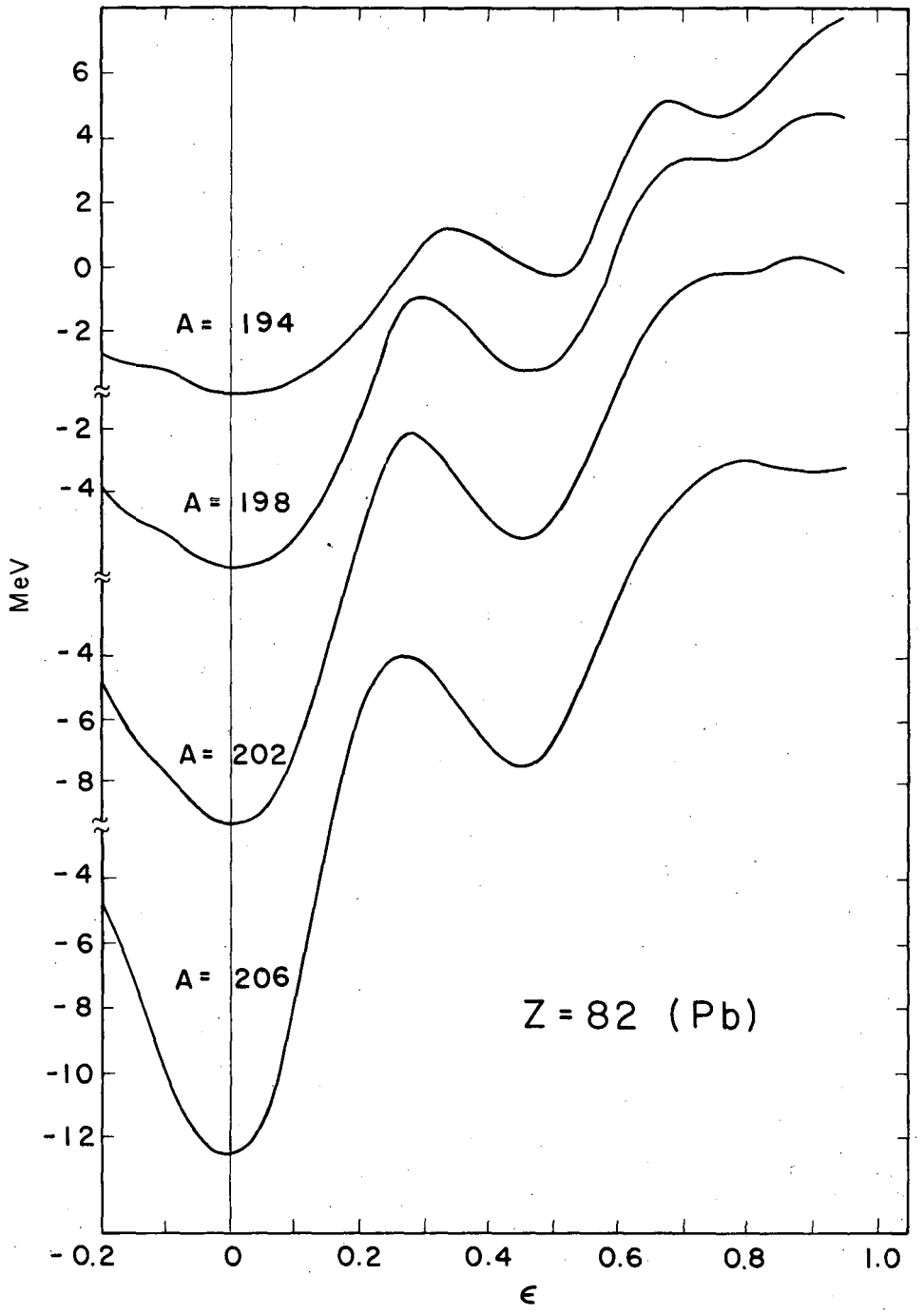

XBL 694-2444

Fig. 11.

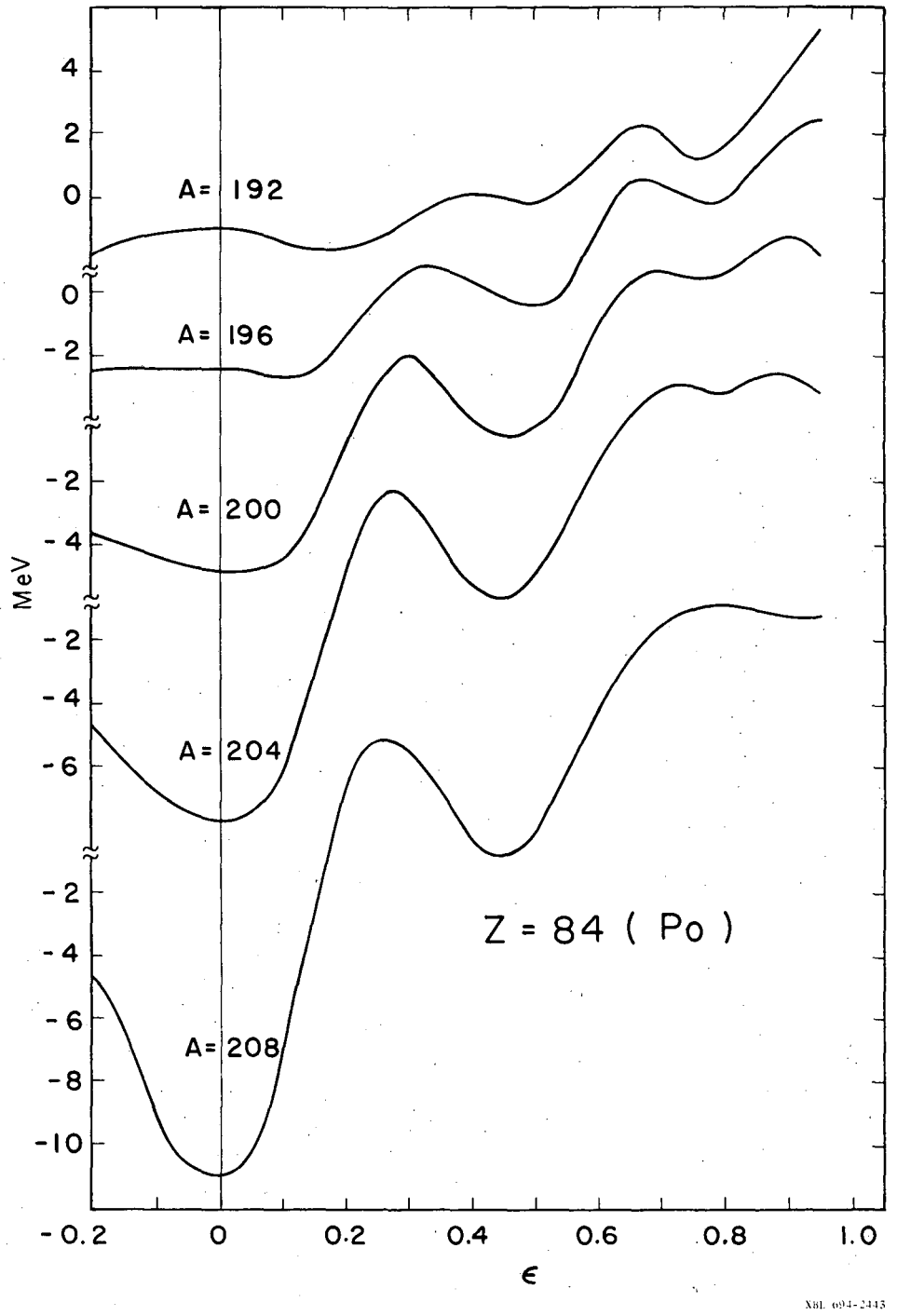
A= 192
A= 196
A= 200
A= 204
A= 208
Z = 84 (Po)
MeV
ε
4
2
0
0
-2
-2
-4
-2
-4
-6
-2
-4
-6
-8
-10
-0.2
0
0.2
0.4
0.6
0.8
1.0
XBL 694-2443

Fig. 12.

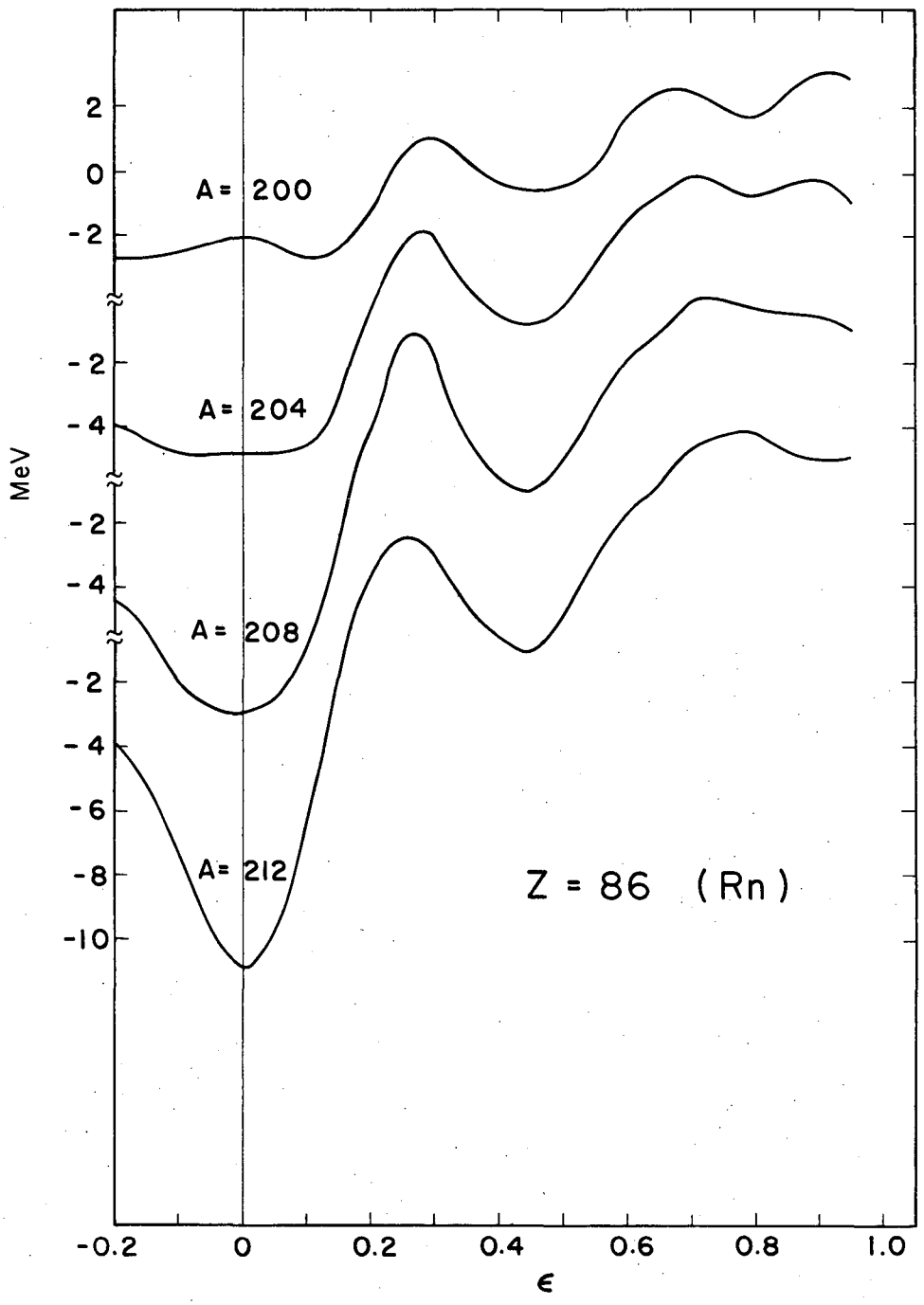

XBL 694-2442

Fig. 13.

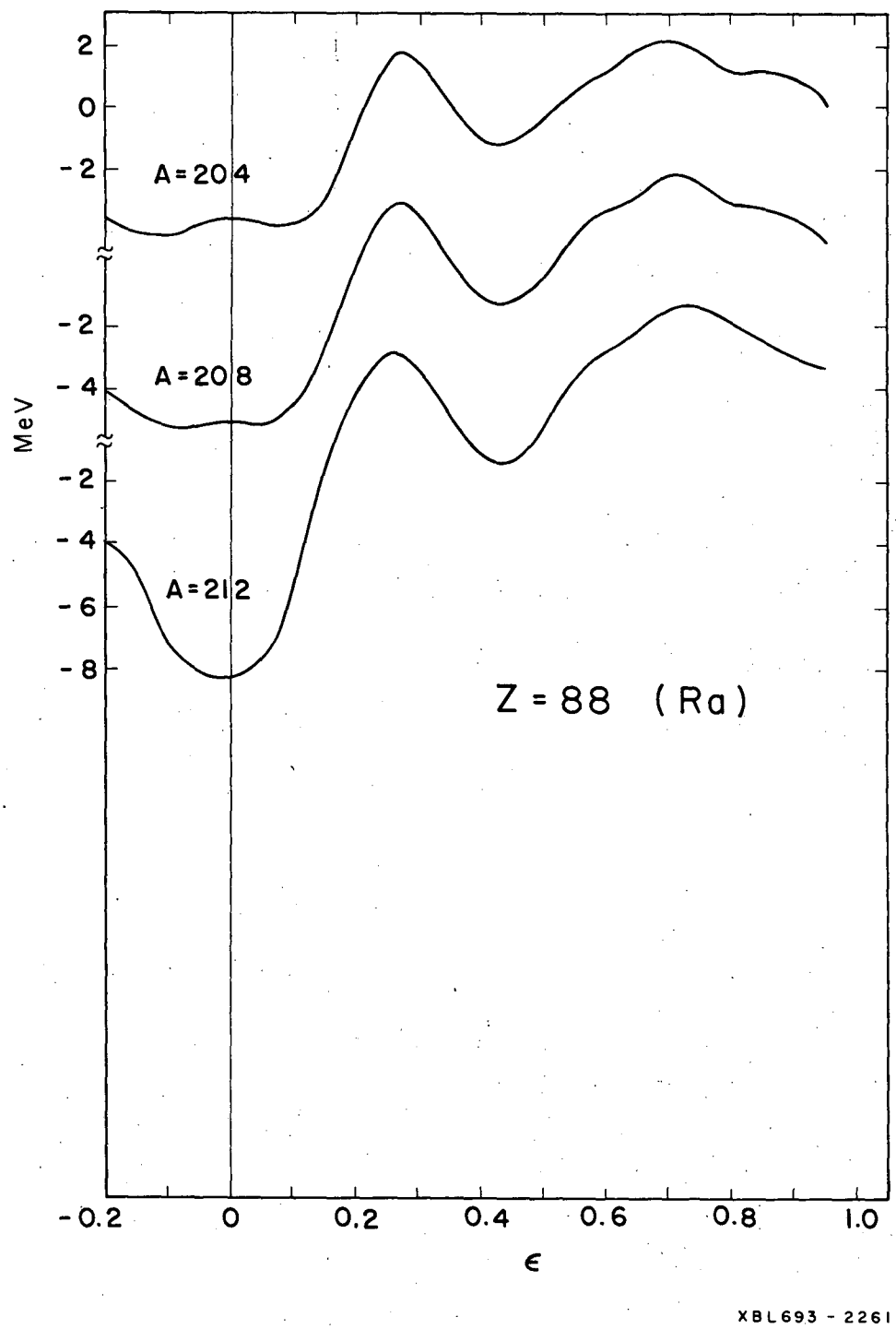
2
0
-2
A=204
-2
-4
A=208
-2
-4
-6
-8
A=212
MeV
Z = 88 (Ra)
-0.2
0
0.2
0.4
0.6
0.8
1.0
ε
XBL693 - 2261

Fig. 14.

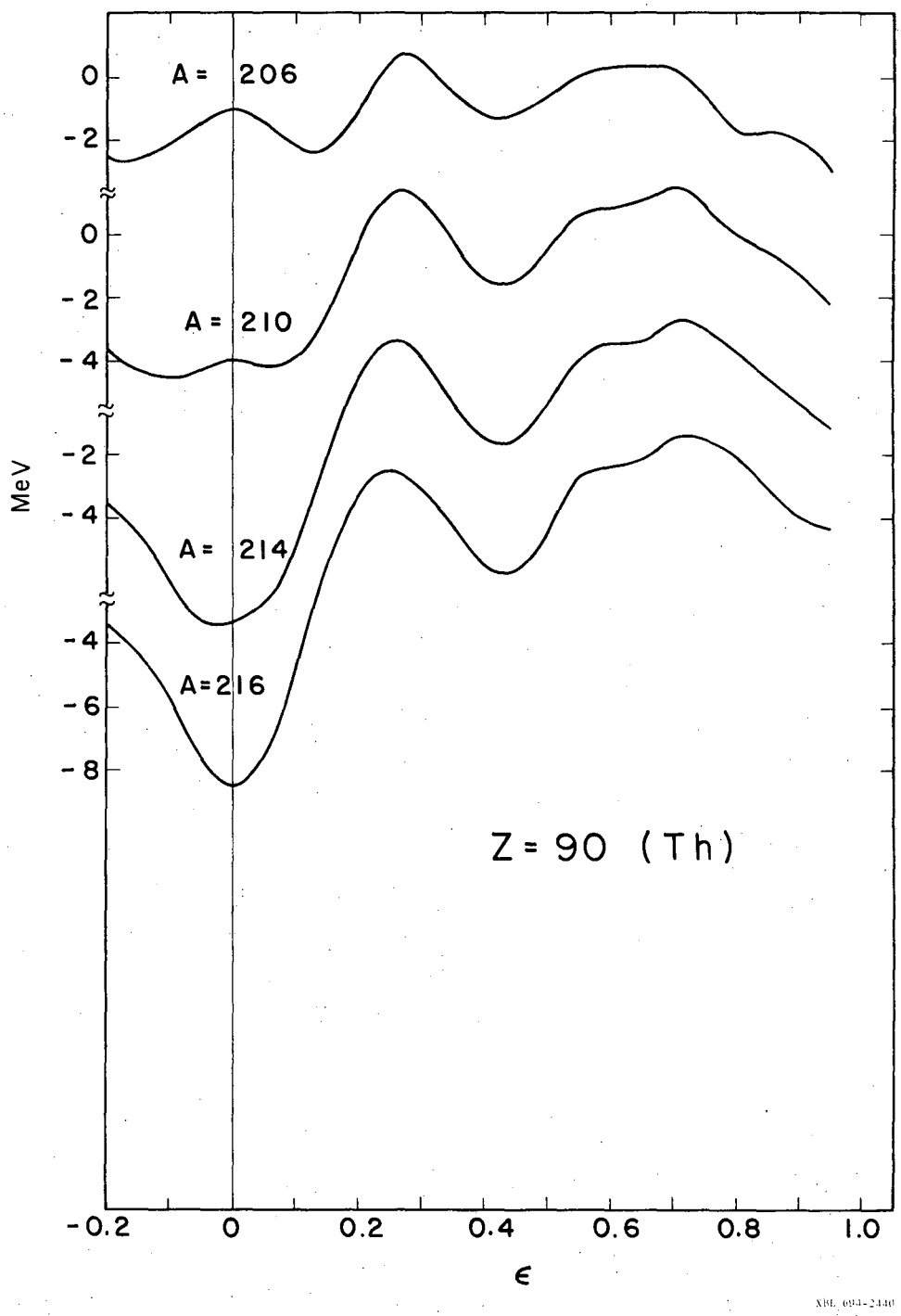

Fig. 15.

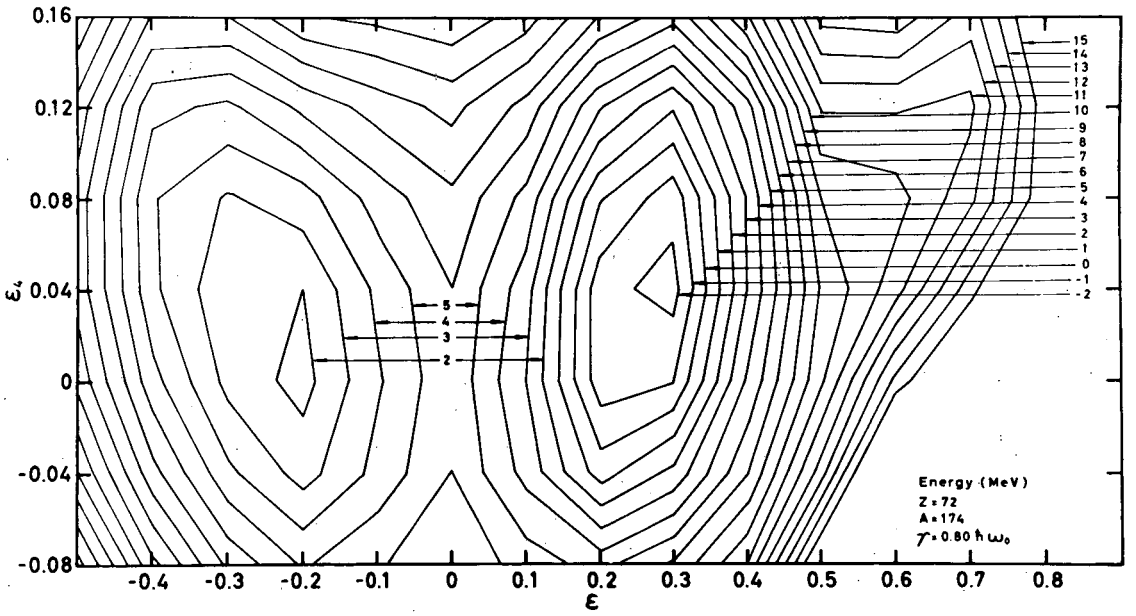

XBL 699-1482

Fig. 16.

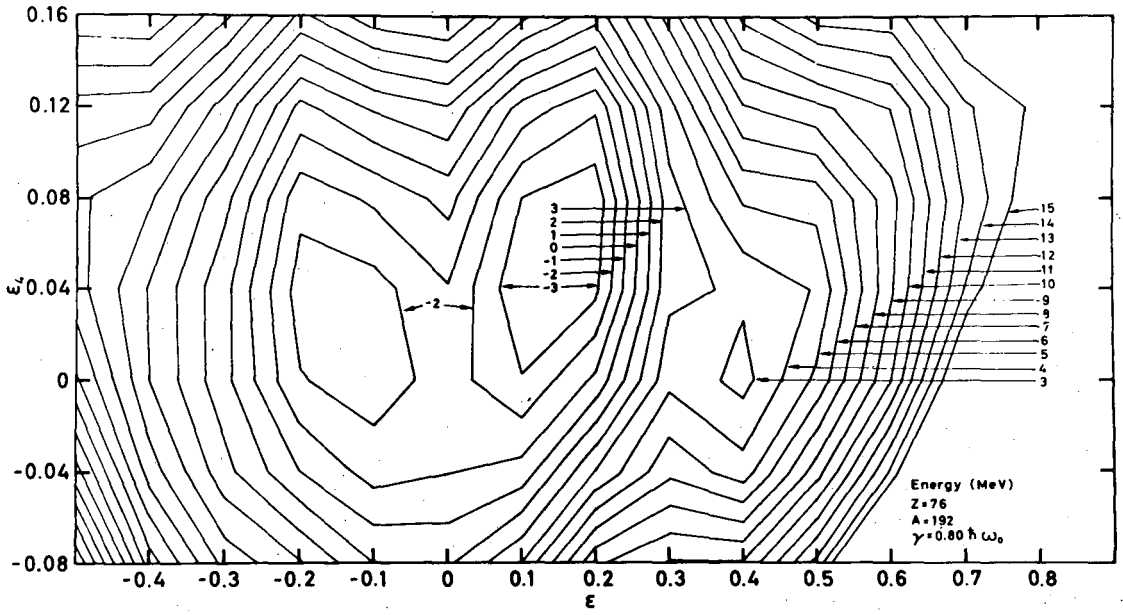

XBL 699-1483

Fig. 17.

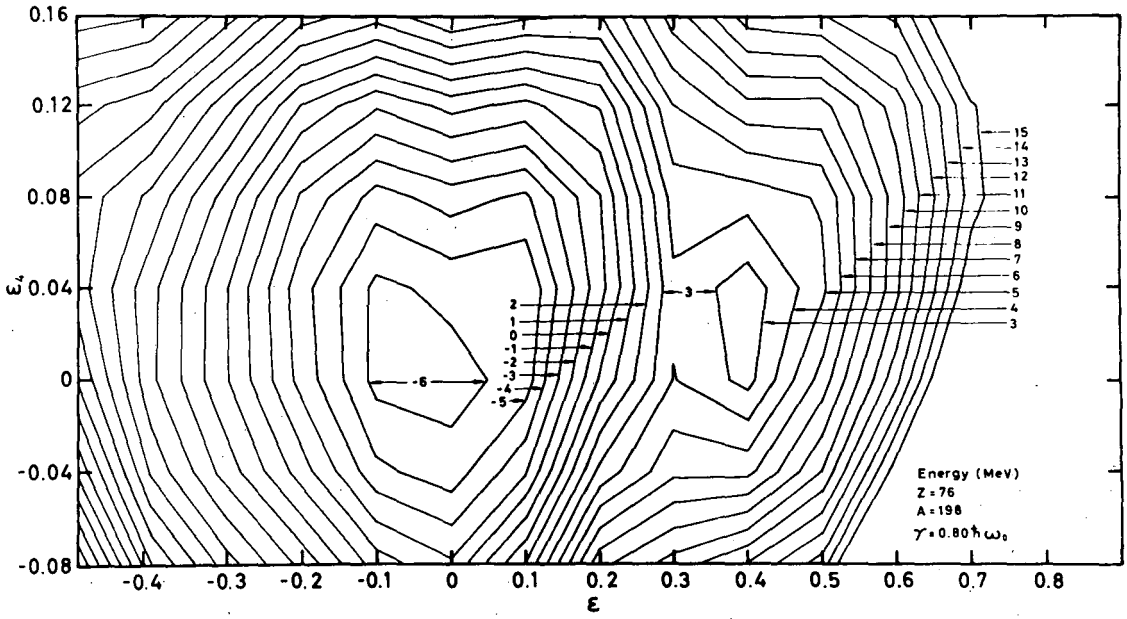

XBL 699-1484

Fig. 18.

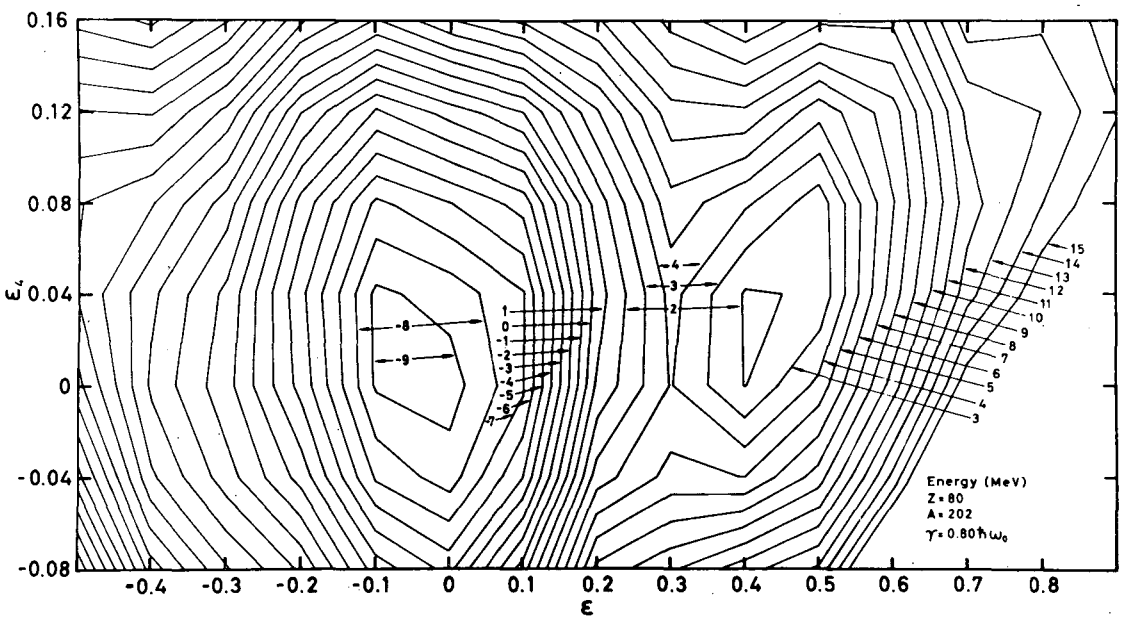

XBL 699-1485

Fig. 19.

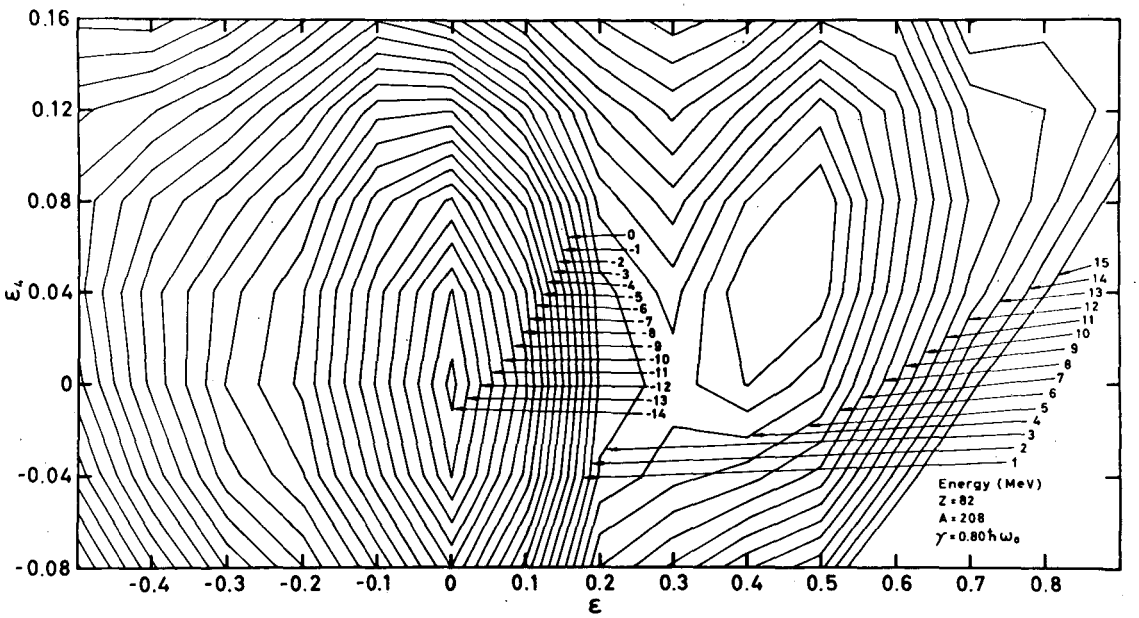

XBL 699-1486

Fig. 20.

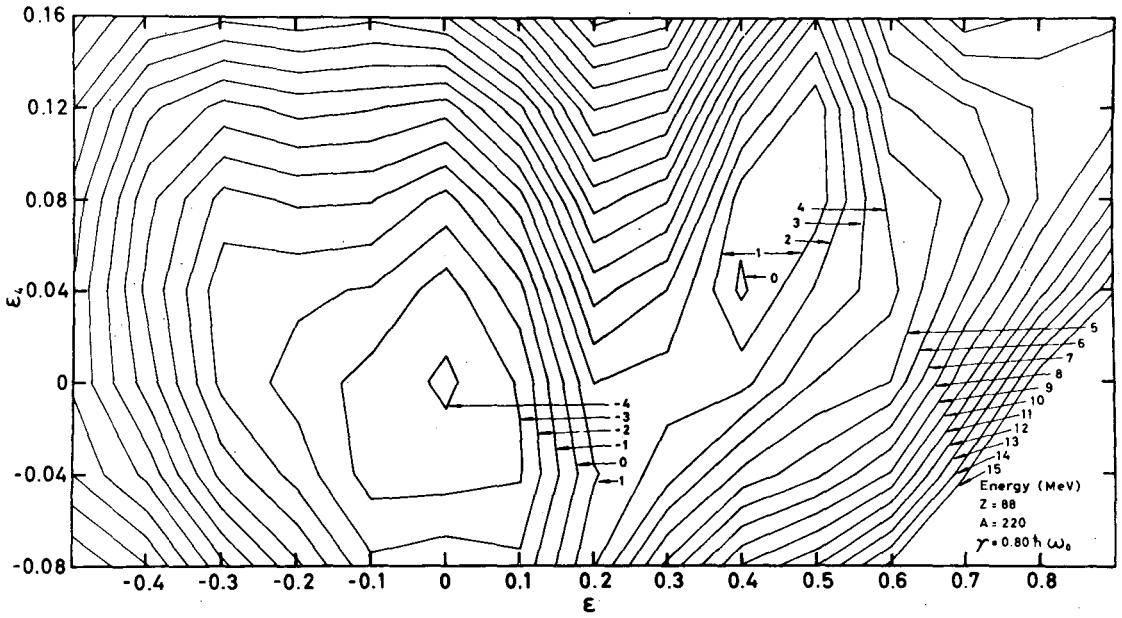

XBL 699-1488

Fig. 21.

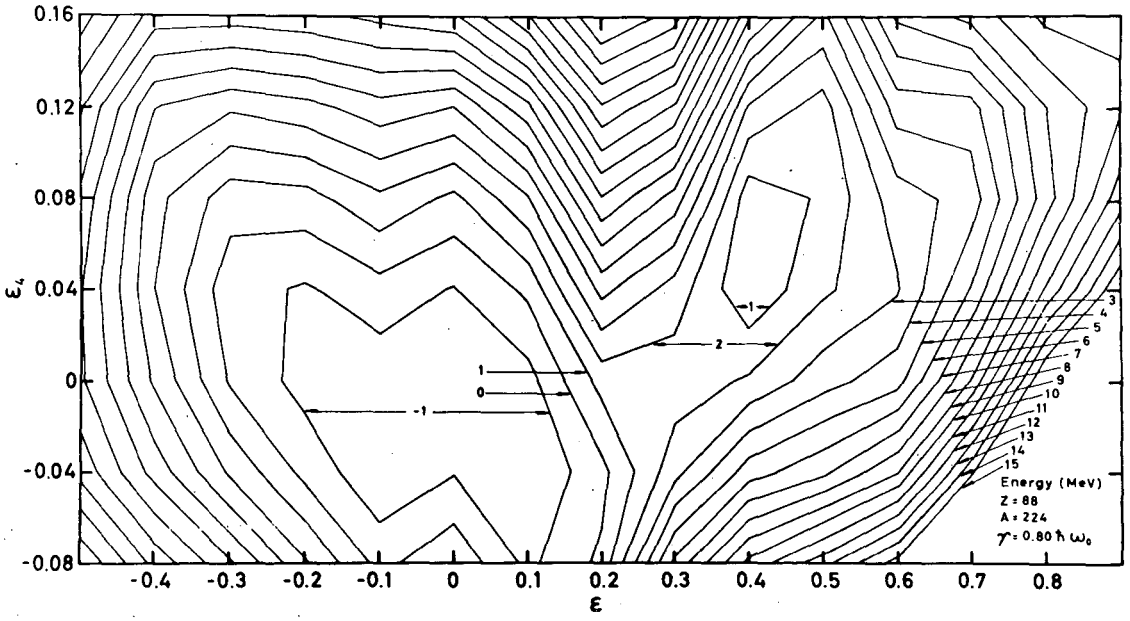

XBL 699-1487

Fig. 22.

LEGAL NOTICE

This report was prepared as an account of Government sponsored work. Neither the United States, nor the Commission, nor any person acting on behalf of the Commission:

A. Makes any warranty or representation, expressed or implied, with respect to the accuracy, completeness, or usefulness of the information contained in this report, or that the use of any information, apparatus, method, or process disclosed in this report may not infringe privately owned rights; or

B. Assumes any liabilities with respect to the use of, or for damages resulting from the use of any information, apparatus, method, or process disclosed in this report.

As used in the above, "person acting on behalf of the Commission" includes any employee or contractor of the Commission, or employee of such contractor, to the extent that such employee or contractor of the Commission, or employee of such contractor prepares, disseminates, or provides access to, any information pursuant to his employment or contract with the Commission, or his employment with such contractor.

TECHNICAL INFORMATION DIVISION
LAWRENCE RADIATION LABORATORY
UNIVERSITY OF CALIFORNIA
BERKELEY, CALIFORNIA 94720